Rapid in Vitro Conformational Changes of the Catalytic Site of PKCα Assessed by FIM-1 Fluorescence†

Agnes Janoshazi* and Jean de Barry

Laboratoire de Neurobiologie Cellulaire, UPR 9009, CNRS, Strasbourg, France

Received February 23, 1999; Revised Manuscript Received June 24, 1999

ABSTRACT: To study the activation process of protein kinase C (PKCα), we used a fluorescent probe, FIM-1, a bis-indolylmaleimide derivative, which binds to the ATP-binding site on the catalytic domain [Chen, C. S., and Poenie, M. (1993) *J. Biol. Chem. 268*, 15812]. This enabled us to directly observe the microenvironment of the ATP-binding site in vitro during the activation process. The FIM-1 binding affinity for PKCα (EC_{50} between 6 and 10 nM) was affected neither by PKCα activating conditions nor by enzyme proteolysis. The fluorescence yield of the PKCα−FIM-1 complex depended on the PKCα activation state. This fluorescence yield was decreased upon proteolysis, which allowed us to study the rate of PKC proteolysis by μ-calpain and its modification by cofactors. Two binding sites were also observed for Ca^{2+} on the partially activated PKCα. After phorbol ester (TPA) application, PKC activation was characterized by biexponential kinetics, including a rapid phase completed within 5 min and a slow phase lasting at least 30 min, which reflected several activation steps. Two different binding sites for TPA were revealed on membrane-associated PKCα (EC_{50} = 31 ± 12 and 580 ± 170 nM), and their modulation by phosphatidylserine and Ca^{2+} was characterized. The high-affinity TPA binding site was highly conserved, even on the soluble enzyme. Our study shows that binding of low concentrations of TPA triggers conformational changes in the soluble PKCα, which affect the microenvironment of its catalytic domain.

Protein kinase C (PKC)[1] is involved in a wide range of signal transduction processes to be triggered by diacylglycerol (DAG) production (*1*). Several groups of PKC isoenzymes are activated in different manners. For the full activation, the conventional (i.e., Ca^{2+}-dependent) cPKC isoforms need to interact with phosphatidylserine (PS) and Ca^{2+} in addition to DAG (*2*). DAG analogues such as phorbol esters can also activate these isoforms (*3*).

All the cPKC isoforms (PKCα, -βI, -βII, and -γ) are comprised of four conserved sequences: C1 and C2 in the regulatory domain and C3 and C4 in the catalytic domain. The regulatory and catalytic domains are connected by a hinge sequence called V3 (*4*). The activity of PKC is kept low in a basal state by the V1 (variable pseudosubstrate) sequence, which is localized at the N-terminus of PKC and binds to the active center of the catalytic domain of the enzyme. The C1 sequence, which is rich in cysteine residues, is responsible for the interaction of the enzyme with DAG in the membrane or with added phorbol esters (*5*−*11*). Two cysteine-rich sequences in the C1 domain have been identified as phorbol ester binding sites (*12*), although these binding sites are not strictly equivalent to the DAG binding sites in the enzyme (*13*, *14*). A recent publication reported that phorbol ester binding sites on C1 are initially hindered on soluble PKCγ, because of the clamping of the V1 pseudosubstrate into the active center of the enzyme (*15*). This fixed conformation of C1 is unfavorable for phorbol ester binding but can be unlocked by releasing the pseudosubstrate V1 from the catalytic site. The binding of the Ca^{2+} and PS cofactors to the C2 sequence, which is responsible for Ca^{2+} and phospholipid regulation (*4*), triggers a conformational change in the C1 sequence. This change exposes both of the phorbol ester binding sites on the C1 sequence (*15*). The role of Ca^{2+} alone in the phorbol ester−PKCα interaction is controversial since several authors reported that phorbol ester binding to PKCα was Ca^{2+}-dependent (*10*, *15*, *16*), while others suggested it was Ca^{2+}-independent (*17*). The PS modulation of the PKC−phorbol ester interaction is well-characterized (*15*, *18*, *19*). However, pre-existing binding sites of phorbol esters on soluble PKC (*18*) and their modulation are still unclear.

The most common feature of all PKC isoforms is that all possess highly conserved catalytic domains C3 and C4 where the ATP and substrate binding sites are located. Despite intense investigation of the involvement of cofactors in the activation process of the enzyme, the events occurring at the catalytic domain during membrane binding and activation of PKC remain poorly understood. It is well-established, however, that the phosphorylation of three sites in the PKC

† This work was supported by Grant ACC-SV12 from the Ministère de l'Enseignement Supérieur, de la Recherche et de la Technologie.

* To whom correspondence should be addressed: Laboratoire de Neurobiologie Cellulaire, UPR 9009 CNRS, 5 rue B. Pascal, F 67084 Strasbourg, France. E-mail: jaja@neurochem.u-strasbg.fr. Telephone: 00 33 3 88 45 66 97. Fax: 00 33 3 88 60 16 64.

[1] Abbreviations: BSA, bovine serum albumin; DAG, diacylglycerol; DMSO, dimethyl sulfoxide; EGTA, ethylene glycol bis(β-aminoethyl ether)-*N*,*N*,*N*′,*N*′-tetraacetic acid; PAGE, polyacrylamide gel electrophoresis; PKC, protein kinase C; PMSF, phenylmethanesulfonyl fluoride; PS, phosphatidylserine; SDS, sodium dodecyl sulfate; SUV, small unilamellar vesicles; TBST, TRIS-buffered saline with 0.2% Triton X-100; TPA, 12-*O*-tetradecanoylphorbol 13-acetate.

10.1021/bi990427m CCC: $18.00
Published on Web 09/14/1999

catalytic domain induces the proper protein alignment for the interaction of C2 sequences with the membrane, which precedes PKC activation (*20*−*25*). According to a recent publication (*25*), the two domains must interact during PKCβ1 membrane binding since C-terminal residue 642 in the catalytic part controls the Ca^{2+} affinity for the C2 sequence.

Several fluorescent probes have been used to investigate the regulatory domain of the enzyme in vitro and in vivo (*14*, *26*−*29*), but few fluorescent probes attached or bound to the catalytic domain were used to study the cofactor activation process of the enzyme (*29*). Hence, the possible conformational change of the catalytic domain during membrane binding and activation by DAG or phorbol ester remained undetected. The development of fluorescent bisindoylmaleimide derivatives as specific PKC competitive inhibitors at the ATP site (*30*, *31*) provides a tool by which the conformational changes of the PKC catalytic domain induced during the different activation processes can be elucidated. Such a probe, FIM-1 (*31*), undergoes a 3-fold fluorescence increase when it is bound to 12-*O*-tetradecanoylphorbol 13-acetate (TPA)-activated PKCα. Here we report that changes in the regulatory domain influence the microenvironment of the ATP site on PKCα since FIM-1 fluorescence intensity varies with the state of activation of PKC by Ca^{2+}, PS, and TPA. We found that the ATP site on the PKCα catalytic domain is unaffected during the activation process by PS, Ca^{2+}, and TPA since the binding affinity of FIM-1 was exceptionally stable. Even the proteolytic form of PKC, called PKM, exhibited an unchanged FIM-1 binding affinity.

This probe allowed us to test PKC under unique conditions, when some of the activation cofactors were excluded, inducing intermediate conformational changes of the partially activated PKC. Two distinct Ca^{2+} binding sites were identified on the membrane-bound but not-fully activated PKCα. We also demonstrated that TPA can bind with soluble PKCα without binding of the protein to membrane lipids, and that these interactions affect the catalytic domain conformation. We identified a high-affinity TPA binding site on the soluble enzyme and studied its modulation by Ca^{2+} and PS. Furthermore, fluorescence measurements also allow rapid kinetic studies starting at the addition of the activator, which are not possible with biochemical methods. Here we report that TPA binding to PKCα exhibits biexponential PS-dependent kinetics, which has not been previously described.

These results bring new important insights to the activation and inactivation processes of conventional PKCs.

EXPERIMENTAL PROCEDURES

Materials. PKCα was a purified recombinant protein obtained from a rabbit clone expressed in a baculovirus expression system and provided by Gibco Life Technologies (Gaithersburg, MD). In some experiments, human recombinant PKCα from Calbiochem (San Diego, CA) was also used. For proteolysis studies, rat brain PKC and PKM were purchased from Gibco Life Technologies. FIM-1 potassium salt was from Teflabs (Austin, TX) and Molecular Probes (Eugene, OR). L-α-Phosphatidyl-L-serine (PS) from bovine brain, TPA, staurosporine and histone H1 (type III), and the polyclonal rabbit antibody against the C-terminal V5 region of rat PKCα (amino acids 659−672) were from Sigma (St. Louis, MO). [γ-^{32}P]ATP was from New England Nuclear (Boston, MA). All other reagents were analytical grade.

Lipid Vesicle Preparation. PS small unilamellar vesicles (SUV, 30 nm) were prepared by dissolving pure PS in chloroform. The solvent was removed under a stream of argon. PS was then dispersed in 20 mM TRIS buffer (pH 7.4) containing 0.1 mM EGTA. PS SUV were formed by tip pulse sonicating (2 s on, 3 s pause) the solution for 3 × 30 s. The output of the tip was 50% of the maximum power (Branson Sonic Power). This preparation was used to maximize PKCα activity, which is modulated by vesicle curvature (*32*).

Spectrofluorimetry. Fresh FIM-1 solutions were prepared on the day of the experiment. FIM-1 was first solubilized in DMSO (280 μM stock solution) and then diluted in the experimental buffer. The spectra were measured in TRIS buffer (20 mM, pH 7.4) using a SLM 48000 or PTI AlphaScan spectrofluorimeters (excitation wavelength of 485 nm, bandwidth of 2 nm). Emission spectra were recorded between 500 and 650 nm (four to six spectra were averaged). Typically, 0.25 μg of purified PKCα was diluted in 1 mL of TRIS buffer (containing different concentrations of Ca^{2+}, EGTA, TPA, and PS vesicles) at 25 °C in a micro quartz cuvette with a path length of 1 cm. After spectral correction of the contribution from the buffer, the light scattering effect, and the slight artifact of the lipid−FIM-1 interaction, the resultant fluorescence spectra were deconvoluted with three Gaussian peaks. Spectra were normalized with respect to a reference spectrum, in most cases (unless otherwise stated) that of PKCα, with 3 nM FIM-1 in TRIS buffer (containing the given amount of PS vesicles in the series). The intensities of the three calculated peaks were divided by that of the corresponding peak in the reference spectrum. The conditions with respect to FIM-1 and PKC concentrations were experimentally adjusted to the optimal signal/noise ratio of the measured fluorescence signal, taking into account the instrumental limitations.

Kinetic Measurements. The limit of the best time resolution was the scanning time of the whole fluorescence spectrum, which was around 10 s. To improve the signal/noise ratio, we averaged between four and ten spectra when needed. The intensities of the first peak were calculated by deconvoluting the averaged spectra. The first data point for rapid TPA binding kinetics was collected 10 s after TPA addition.

Biochemical Assay of PKCα Activity. PKCα activity was determined by the extent of histone phosphorylation. PKCα was mixed with different amounts of FIM-1 for the inhibitory test or a fixed concentration (3 nM) for the TPA dependence study. PKCα aliquots (0.1 μg of purified protein) were incubated for 20 min at 30 °C in 20 mM TRIS buffer (pH 7.4), containing 5 mM $MgCl_2$, 1 mM EGTA, 2.5 mM $CaCl_2$, 20 μM ATP, 2 mM PMSF, histone H1 (2 mg/mL), and [γ-^{32}P]ATP (3×10^5 cpm, specific activity of 110 TBq/mmol), in a final volume of 100 μL. This incubation solution contained either 120 nM TPA (for the FIM-1 inhibitory test) or a different amount of TPA (for the TPA dose−response assay). Aliquots (30 μL) of the reaction mixture were then dotted on cation exchange chromatography paper (P81, Whatmann International, Maidstone, England). The paper was subsequently washed three times with trichloroacetic alcohol and then dried. Radioactivity was measured by the

Cerenkov method using a SL-6000 scintillation counter (Beckman Instruments, Palo Alto, CA). The assay was performed in the absence (basal activity) or in the presence of 170 μg/mL PS (inducible activity).

Proteolysis by μ-Calpain, Assessed with Western Blots. Proteolysis was carried out with activated PKCα (2 μg/mL), which was previously incubated with 125 nM TPA for 30 min at 25 °C in 20 mM TRIS buffer (pH 7.4) containing 2 mM $CaCl_2$ and 70 μM PS vesicles (final volume of 1 mL). By starting the proteolysis with the addition of μ-calpain (4.1 units) to the solution and mixing vigorously at 25 °C, we could follow the process by taking out 30 μL aliquots at given time intervals. To stop the proteolysis, samples were frozen in liquid nitrogen. Samples were analyzed by SDS−PAGE on 4 to 20% gradient gels (Miniprotean Ready Gels, Bio-Rad), and the protein blotting was subsequently achieved with PVDF membranes (Immobilon, Millipore). After blocking for 4 h in TRIS-buffered saline (pH 7.2) containing 0.01% Tween 20 and 1% BSA (TBST/BSA), the blots were incubated overnight with a polyclonal antibody (1 ng/mL) raised in rabbits against a synthetic peptide corresponding to the N-terminus of the catalytic domain of a rat PKCα isoform (Sigma). They were then washed (4 × 30 min) in TBST/BSA and incubated for 30 min with a goat anti-rabbit antibody conjugated to horseradish peroxidase (diluted 1/500, Sigma). After being washed (4 × 15 min in TBST), the immunoblots were revealed using the Super Signal substrate (Pierce, Rockford, IL) and ECL-Hyperfilm (Amersham, Buckinghampshire, U.K.). A subsequent quantification of the blots was performed using a computer image analyzer (Starwise, Imstar, Paris, France). Blanks were obtained using the primary antibody in the presence of the antigen peptide (1 μg/mL). Western blotting, immunoreaction, and quantification were performed at least twice for each sample. The linearity of the response was checked using a serially diluted homogenate.

Determination of Free Ca^{2+} Concentrations. Free Ca^{2+} concentrations were calculated by using a computer program written by J. L. Rodeau that takes into account pH and Ca^{2+}, Mg^{2+}, K^+, Na^+, and EGTA concentrations. This program was based on the calculation of McGuigan et al. (*33*). We always refer to the free Ca^{2+} concentrations.

Fit and Statistics. Deconvolution of multicomponent spectra was accomplished by an iterative nonlinear least-squares technique based on the Gauss−Newton method. The normalized values were calculated for each sample, and then the average and the standard deviation (SD) were calculated from the experimental data set of the same batch of the PKC enzyme. The final reported average values and errors (SD) were calculated from the average and standard deviation of each series. The errors of the fitting calculations and of the instrument were negligible compared with the SD values. Dose−response curves were fitted according to one- or two-site models using the *F* test to determine the best model.

RESULTS

Spectral Characterization of FIM-1. FIM-1 is a bis-indolylmaleimide derivative, which specifically binds near the ATP site on the catalytic domain of PKCα. It is structurally related to staurosporine, a well-known kinase inhibitor, which competes with FIM-1 for the ATP site (*31*).

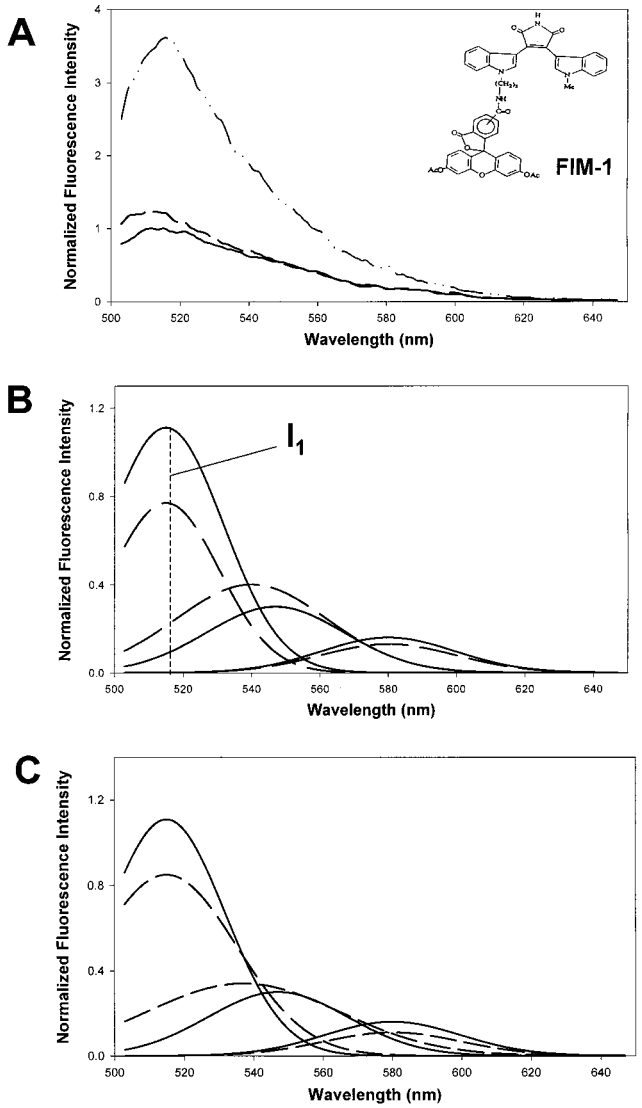

FIGURE 1: Spectral properties of FIM-1. (A) Effect of PKCα and TPA on the FIM-1 raw emission spectrum. FIM-1 (3 nM) was incubated in TRIS buffer (20 mM, pH 7.4) with 1.5 mM Ca^{2+} in the presence of PS small unilamellar vesicles (13 μM) (—), with PKCα (1 nM) (− − −), and with PKCα and 120 nM TPA (− · · −). The spectra were recorded at $E_x = 485 \pm 4$ nm after incubation for 30 min. Note the prominent effect of TPA on FIM-1 fluorescence intensity. The inset shows the chemical structure of FIM-1. (B) Deconvolution into three Gaussian components of the emission spectra of FIM-1 alone (− − −) or in the presence of PKCα (—). This illustrates the subtle spectral distortions, which can be revealed by deconvolution. (C) Effect of staurosporine on FIM-1 fluorescence measured in the presence of PKCα; deconvoluted emission spectra of 3 nM FIM-1 incubated with 1 nM PKCα in the same buffer as described for panel A without TPA (—) and after incubation for an additional 10 min after 200 nM staurosporine was added (− − −).

FIM-1 alone in TRIS buffer exhibits a broad fluorescence spectrum between 500 and 650 nm, with a maximum at 518 nm upon excitation at 490 nm. Its extinction coefficient is 108 000 M^{-1} cm^{-1}.

Fluorescence emission of the probe is slightly enhanced in the presence of soluble purified PKCα (Figure 1A). The probe was extremely sensitive to the activation state of PKC which is reflected by an almost 3-fold increase in the fluorescence intensity when the membrane-bound enzyme was fully activated by phorbol ester (Figure 1A,B). Since the emission spectrum was broad and complex, it suggested

the existence of several emission peaks. Gö7874, which is another bis-indolylmaleimide derivative similar to FIM-1 but has no fluorophore attached to it, exhibits an emission spectrum with a peak at 535 nm upon excitation at 490 nm due to the indolyl residue (not shown). The fluorescein marker itself has an emission peak around 518 nm at this excitation wavelength. These two independent fluorophores suggested that at least two peaks should contribute to the measured emission spectrum. The mathematical analysis of our raw data showed that three Gaussians give the best relevant fit. The three significant peaks were at 518, 535, and 580 nm (Figure 1B). This spectral analysis allowed a more precise quantification of the signal since conformational changes of the enzyme induced changes not only in the integral intensity but also in the shape of the emission spectrum of the probe. However, since two peaks can act differently, e.g., one peak can increase while the other peak decreases its intensity or shifts its maximum (Figure 1C), their sum can mask these changes. The deconvolution enabled us to see fine modulations by following only one of the most sensitive peak changes. One of the best indicators is the integrated intensity of the Gaussians (I). I_1-I_3 were used to determine the affinity of the FIM-1 binding site for PKCα. Identical behaviors of the first and third peaks (I_1 and I_3) were detected under most of the PKC stimulating conditions, but the third peak intensity varied between probes coming from different batches. The second peak (I_2) acted independently from the first, shifting to the longer-wavelength region of the spectrum (as seen in panels B and C of Figure 1). The I_1 peak was the most prominent and fundamental peak, which had a practically stable maximal wavelength around 518 nm. To simplify the method, we use only the integral intensity of this first peak I_1 as one of the indicators of the spectral changes. The following data are always referring to I_1.

Characterization of the FIM-1−PKCα Interaction. In the presence of 2 mM Ca^{2+}, the PKCα−FIM-1 interaction occurred very rapidly as observed by a small but detectable fluorescence increase with a time constant of <100 ms measured at $E_m = 518 \pm 4$ nm with a rapid stop-flow apparatus ($E_x = 485 \pm 4$ nm). Steady-state spectral data showed that FIM-1 had a higher fluorescence yield when it bound to lipid-associated PKCα. A 3-fold maximal increase in fluorescence was achieved with fully activated PKCα by TPA (it increased to more than 10-fold with the rat brain PKC preparation from Gibco). When staurosporine was subsequently added to the mixture of FIM-1 and soluble PKCα, it partially reversed the spectral changes of the FIM-1−PKC complex by competing for the same binding site (Figure 1C).

The fluorescence intensity of the probe dose-dependently increased with FIM-1 concentration in the presence of a fixed PKCα concentration (Figure 2). The EC_{50} value of FIM-1 binding curves was unaffected or slightly modulated according to the presence of PKCα activators acting separately or together on the regulatory domain of the enzyme (Figure 2 and Table 1). The Hill coefficient (n_H) for all the measured dose−response curves was consistently around 2 (Table 1). The fluorescence intensity increased significantly when Ca^{2+} and/or PS was added to the medium. The amplitude change was maximal (an almost 3-fold increase) in the presence of PS, Ca^{2+}, and TPA, three agents which trigger complete

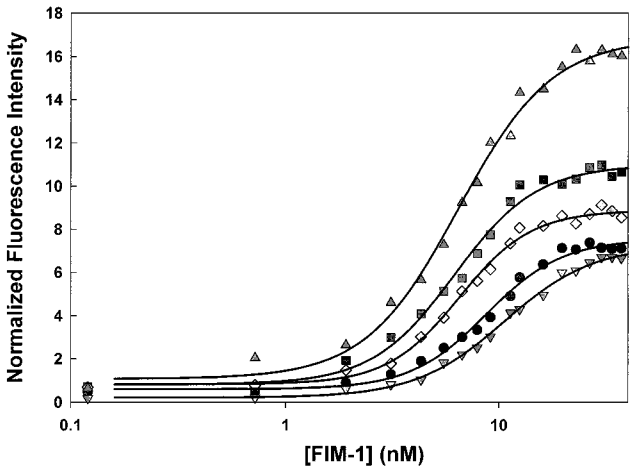

FIGURE 2: Curves for FIM-1 binding to PKCα in the presence of different activation cofactors. FIM-1 at various concentrations was incubated in 20 mM TRIS buffer (pH 7.4) at 25 °C for 5 min in the absence of PKCα or in the presence of 3 nM PKCα and various cofactors. Fluorescence spectra were recorded between 500 and 650 nm at $E_x = 485 \pm 4$ nm and deconvoluted. For each FIM-1 concentration, the emission intensity of the first Gaussian peak (I_1) measured in the presence of FIM-1 alone was subtracted from the I_1 values measured in the presence of PKCα and the various cofactors (corrected I_1). The corrected I_1 values were then normalized with the corrected I_1 value measured in the presence of 3 nM FIM-1 and 3 nM PKCα in the absence of cofactors (standard conditions). This peak intensity was taken as a unit. The recording experimental conditions were as follows: PKCα alone (●), PKCα preincubated for 5 min with 13 μM PS vesicles (■), PKCα with 1.5 mM Ca^{2+} (■), PKCα preincubated for 5 min with 13 μM PS vesicles and 1.5 mM Ca^{2+} (▼), and PKCα preincubated for 30 min with 120 nM TPA in the presence of 13 μM PS vesicles and 1.5 mM Ca^{2+} (△). Data represent the average of two series of three independent experiments ± SD.

Table 1: FIM-1 Affinities and Hill Coefficients[a]

Ca^{2+}	PS	TPA	EC_{50} (nM)	n_H
without	without	without	8.72 ± 0.59	2.44 ± 0.18
without	with	without	10.58 ± 0.20	2.09 ± 0.26
with	without	without	6.19 ± 0.80	2.24 ± 0.21
with	with	without	6.52 ± 0.81	2.57 ± 0.30
with	with	with	6.46 ± 1.06	1.98 ± 0.20

[a] FIM-1 (3 nM) fluorescence was measured in the presence of 3 nM PKCα after incubation for 5 min in TRIS buffer (20 mM, pH 7.4). When present, the concentration of Ca^{2+} was 1.5 mM, PS 13 μM, and TPA 120 nM. These data are representative of four independent experiments ± SD.

PKCα activation (Figure 2). To eliminate the possibility of any artifact, the probe fluorescence was measured in the presence of the different cofactors and in the absence of the enzyme. FIM-1 had no direct interaction with either Ca^{2+} or TPA at the concentrations used in this study (not illustrated). A slight quenching effect was observed when the experiment was performed in the presence of PS vesicles at concentrations of >10 μM (Figure 2), indicating a slight but direct FIM-1 interaction with PS.

To verify the specificity of FIM-1 binding to PKCα as measured by fluorescence (*31*), we also checked its inhibitory effect on histone phosphorylation by PKC. We performed biochemical measurements of PKCα activity with 120 nM TPA and 2 mM Ca^{2+} in the presence of PS vesicles with varying FIM-1 concentrations. As expected, FIM-1 inhibited PKCα phosphorylating activity (Figure 3) with an IC_{50} of 13.3 ± 0.8 nM, a value closely consistent with those

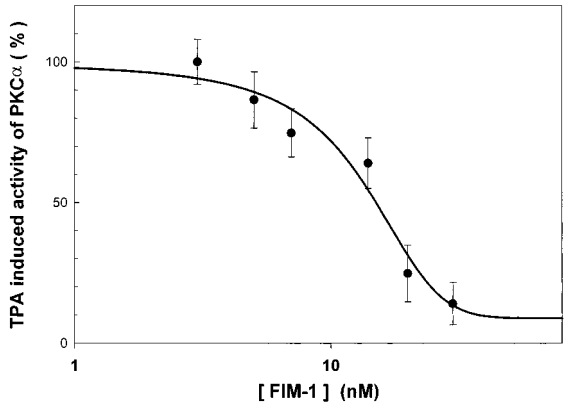

FIGURE 3: Inhibition of PKCα phosphorylating activity by FIM-1. PKCα (0.25 μg/mL) was previously mixed with different amounts of FIM-1 before performing the radioactive assay as described in Experimental Procedures. $IC_{50} = 13.3 \pm 0.8$ nM. Data represent the average of two series of two independent experiments ± SD.

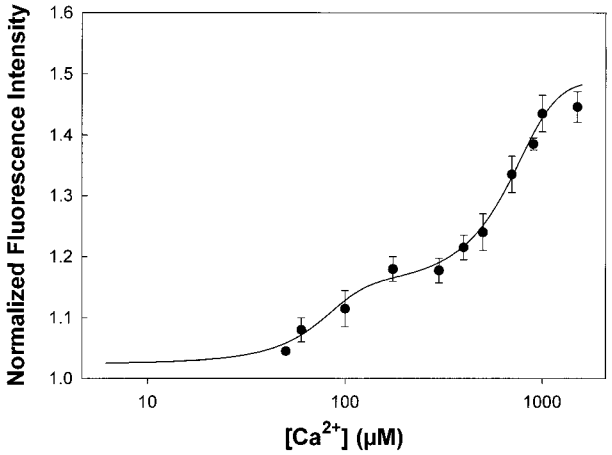

FIGURE 4: Ca^{2+} concentration dependence of the fluorescence of the PKC−FIM-1 complex. Human recombinant PKCα (0.25 μg/mL) was labeled with 3 nM FIM-1 and then incubated with 1 μM PS vesicles in 20 mM TRIS buffer at 25 °C with various Ca^{2+} and EGTA concentrations. The free Ca^{2+} concentration ranged from 40 to 1200 μM. The data are the average of four series of two independent experiments ± SD.

determined by the fluorescence method (Table 1). In this case, the n_H value was close to 1.5.

Characterization of the Ca^{2+}−PKCα Interaction. We addressed two questions: does the inactivated or slightly activated form of PKCα exhibit any detectable conformational change during Ca^{2+} binding, and if so how many Ca^{2+} binding sites participate in this change? We investigated the Ca^{2+} dependence of the fluorescence increase using FIM-1-labeled human recombinant PKCα (3 nM) (Calbiochem). To minimize the direct interaction of FIM-1 with PS lipid vesicles, we lowered the PS concentration to 1 μM. We measured the Ca^{2+} dose dependency in the absence of phorbol ester activator. A clear Ca^{2+} dose-dependent fluorescence increase (Figure 4) for Ca^{2+} concentrations ranging from 40 to 1200 μM was observed. The dose-dependent curve suggested that two distinct Ca^{2+} binding sites on PKCα initiated the observed fluorescence changes ($p < 10^{-4}$ when compared to a one-site model with the F test) with EC_{50} values of 65 ± 23 and 531 ± 30 μM ($n = 5$). Ca^{2+} binding affected the catalytic domain of the partially membrane-bound enzyme, suggesting a global conformational change of the protein.

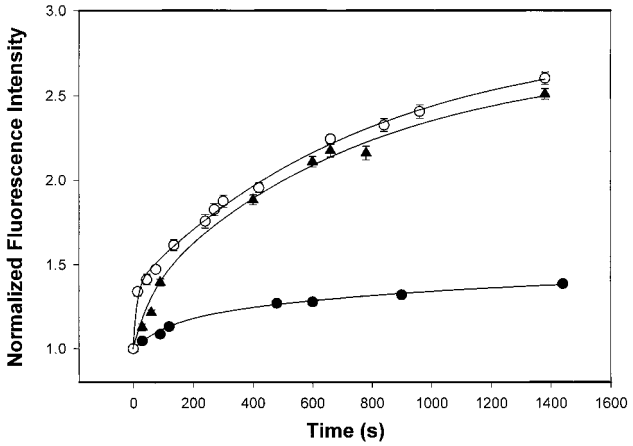

FIGURE 5: Kinetics of the TPA-induced fluorescence increase of FIM-1-labeled PKCα at various PS concentrations. PKCα (0.25 μg/mL) was labeled with 3 nM FIM-1 in TRIS buffer containing 2 mM Ca^{2+} and preincubated with different amounts of PS vesicles for 5 min at 25 °C before the addition of 620 nM (final concentration) TPA. After deconvolution of the spectra, I_1 intensities were normalized by I_1 ($t = 0$ s) and plotted vs time. The phorbol ester-induced fluorescence increase (I_1) was time-dependent. Kinetics recorded in the presence different PS concentrations are presented: PS, 56 nM (●); PS, 70 μM (▲); and PS, 140 μM (○). The rate and the amplitude of the fluorescence change induced by the TPA−PKCα interaction depend on the PS concentration. Data represent the average of four series of two independent experiments.

Characterization of TPA−PKCα Interactions and Their Modulation by PS. The interaction of the phorbol ester TPA with PKCα was assessed in the presence of 2 mM Ca^{2+} with or without PS. PS concentrations of 56 nM, 70 μM, and 140 μM were used to give a wide range of PS concentrations that would completely saturate the PS binding sites on PKC (*16*). We first estimated the time required for the effect of the addition of 70 μM PS to the PKCα−FIM-1 complex (without TPA). A monoexponential increase in FIM-1 fluorescence was measured with a time constant of 69 ± 1 s (not shown). This weak (2%) increase represented the PKC−PS interaction since a direct effect of PS on FIM-1 resulted in quenching of the fluorescence (see above). Hence, to assess the TPA interaction with PKCα, we used equilibrated PS vesicles associated with PKC in the presence of FIM-1 after preincubation for 600 s before adding TPA to the medium.

Binding of TPA to soluble or membrane-associated PKCα induced a FIM-1 emission intensity increase, which was not complete after 30 min (Figure 5). In the absence of PS vesicles, the interaction of 100 nM TPA with 3 nM soluble PKC induced a slow and weak (5%) increase in FIM-1 fluorescence with a single exponential ($\tau = 546 \pm 27$ s, not illustrated). This slow time constant indicates that the binding site on the soluble PKC cannot be easily accessed by TPA. The presence of PS changed the TPA-induced binding kinetics to biphasic. Even a very low PS vesicle concentration (56 nM) resulted in the appearance of a second, faster component, the graph now exhibiting at least two exponentials with distinct rates for the fluorescence increase (Figure 5). The fast rate kinetics became evident with high PS concentrations (Figure 5). Not only was the amplitude of this fast kinetic response enhanced with higher PS concentrations, but the time constant was also dramatically decreased, indicating the dominant PS involvement in this kinetic scheme (Table 2). In contrast, the PS concentration did not

Table 2: PS Dependence of the Time Constants and Amplitudes of the TPA−PKC Interaction[a]

[PS] (μM)	τ_1 (s)	amplitude$_1$	τ_2 (s)	amplitude$_2$
0.056	113 ± 34	0.15 ± 0.09	1002 ± 101	0.25 ± 0.04
70	45 ± 8	0.39 ± 0.05	734 ± 80	1.11 ± 0.02
140	13 ± 5	0.47 ± 0.04	708 ± 98	1.29 ± 0.0

[a] The PKCα− FIM-1 complex was equilibrated with the given amount of PS vesicles [in 20 mM TRIS-HCl buffer (pH 7.4) with 2 mM Ca^{2+}] 300 s before adding 620 nM TPA. The fluorescence spectra were recorded immediately after TPA addition. The average of four series of two independent experiments was analyzed.

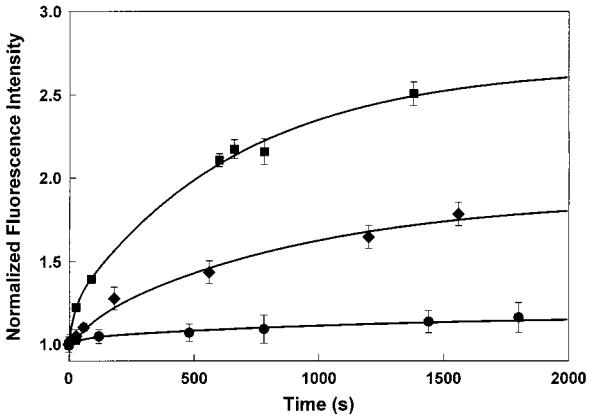

FIGURE 6: Kinetics of the TPA-triggered fluorescence increase of FIM-1-labeled PKCα in the presence of different TPA concentrations. FIM-1 (3 nM) was mixed with PKCα (0.25 μg/mL) and 2 mM Ca^{2+} [in 20 mM TRIS-HCl buffer (pH 7.4)] and incubated at 25 °C with 70 μM PS vesicles for 5 min prior to TPA addition. Various TPA concentrations such as 10 (●), 100 (◆), and 620 nM (■) were added at time zero to the incubation medium. Spectra were then recorded at the indicated times. The kinetics are presented and fitted with two exponentials ($p < 10^{-4}$). Both time constant values are dependent upon TPA concentration. Data are the average of five series of two independent experiments ± SD.

Table 3: TPA Dependence of the Time Constants and Amplitudes of the TPA−PKC Interaction[a]

[TPA] (nM)	τ_1 (s)	amplitude$_1$	τ_2 (s)	amplitude$_2$	$\tau_1/\tau_2 \times 10^{-2}$
10	89.0 ± 4.0	0.06 ± 0.01	1300 ± 62	0.17 ± 0.05	6.8 ± 0.5
30	72.7 ± 16.0	0.07 ± 0.05	1100 ± 75	0.30 ± 0.040	6.6 ± 1.5
100	65.5 ± 5.0	0.18 ± 0.02	799 ± 141	0.61 ± 0.05	8.2 ± 1.6
620	43.0 ± 14.0	0.48 ± 0.04	570 ± 75	1.13 ± 0.04	7.5 ± 2.6

[a] FIM-1 (3 nM) was mixed with PKCα (0.25 μg/mL) and 2 mM Ca^{2+} [in 20 mM TRIS-HCl buffer (pH 7.4)] and preincubated at 25 °C with 70 μM PS vesicles for 5 min before adding TPA to the preparation. Data are the average of five series of two independent measurements.

significantly affect the second, slow kinetic rate, although its amplitude was enhanced by high PS concentrations (Table 2).

TPA Concentration Dependence of Biexponential Kinetics. Several TPA concentrations were used to study the TPA-triggered kinetics as shown in Figure 6. The changes of the fluorescence intensities were best fitted with two exponentials. The two time constants differed by more than 1 order of magnitude (Table 3). They were both similarly affected by TPA since their ratio remained nearly constant, when the TPA concentration varied from 10 to 620, suggesting that a similar reaction sequence or a common step modified both rates (Table 3). To gain some clue about the steps contributing to the observed rates, the two rate values were plotted

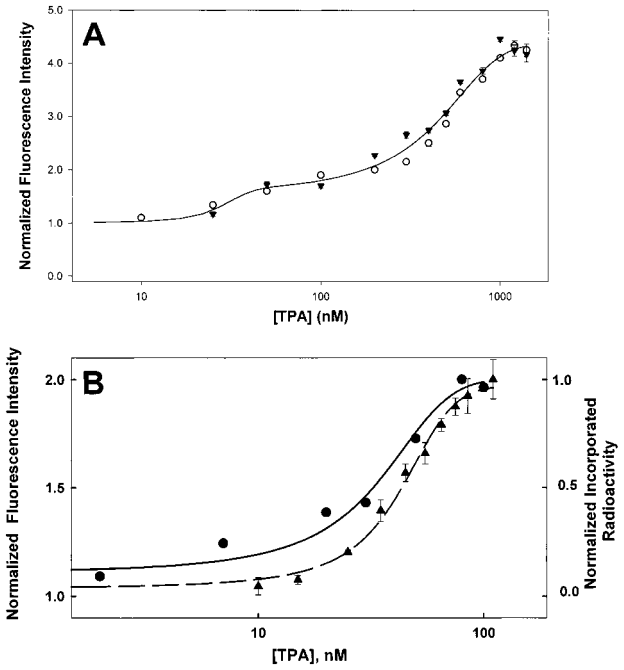

FIGURE 7: Dose-dependent TPA fluorescence increase of the PKCα−FIM-1 complex. (A) Two TPA binding sites on PKCα bound to lipid vesicles. Steady-state fluorescence spectra were recorded after incubation for 5 min with various TPA concentrations in the presence of PS-equilibrated PKCα (0.25 μg/mL) labeled with 3 nM FIM-1, in 20 mM TRIS buffer (pH 7.4) at 25 °C containing PS vesicles (70 μM) and 2 mM Ca^{2+}. The graph represents two series of three independent experiments performed with PKCα from two different sources [Gibco Life Technologies (▼) and Calbiochem (○)] Errors bars represent the SD. (B) Comparison of high-affinity TPA binding on FIM-1-labeled PKCα using fluorescence measurements (dashed line and ▲) or phosphorylating activity (solid line and ●). The fluorescence measurements were performed under the same conditions described for panel A, except that the buffer contained a lower PS concentration (13 μM PS vesicles). Normalization was performed from I_1 recorded in the absence of TPA. The extent of ^{32}P incorporation in histone I was measured by incubating the PKCα−FIM-1 complex at 30 °C for 20 min as described in Experimental Procedures. The graph depicts data from four series of two separate experiments ± SD.

versus TPA concentrations. Both curves showed the involvement of two TPA−PKC binding sites (not shown). Since both rates were TPA concentration-dependent, the most probable contributing steps were the TPA binding to PKCα and/or the following conformational changes of the protein complex (Table 3).

TPA Binding Affinities and the Effect of PS and Ca^{2+}. Since not only the rates but also the amplitudes of the fluorescence signal were sensitive to TPA concentration, we have chosen the change in the amplitude to study the TPA dependence. Furthermore, the enzyme stability limited the duration of our experimental protocol, and our period of observation for the TPA-induced fluorescence change was not longer than 300 s. Due to this period of observation, the relative contribution of faster rate kinetics was prominent compared to the additional signal of the slow kinetics. We used this condition as a pseudo "equilibrium". This equilibrium assumption was justified by the fact that the ratio of the two rates was not sensitive to the change in TPA concentrations, so their proportional contribution to the measured signal was steady. (Table 3). The effect of TPA concentration on PKCα−FIM-1 complex was measured in the range of 4−1200 nM at 25 °C in the presence of 70 μM

Table 4[a]

(A) Effect of Ca^{2+} Concentration on TPA Affinity and FIM-1 Fluorescence Intensity

$[Ca^{2+}]$ (μM)	EC_{50} (nM)	amplitude
0	35.9 ± 1.2	0.05 ± 0.01
125	35.5 ± 2.4	0.11 ± 0.02
500	55.5 ± 3.1	0.21 ± 0.02

(B) Effect of PS Concentration on TPA Affinity and FIM-1 Fluorescence Increase

		TPA			
[PS] (μM)	$[Ca^{2+}]$ (μM)	EC_{50}^1 (nM)	amplitude$_1$	EC_{50}^2 (nM)	amplitude$_2$
0.3	1000	31 ± 5	0.21 ± 0.02	−	−
0.5	1000	34 ± 3	0.27 ± 0.02	−	−
1	1000	38 ± 4	0.33 ± 0.02	−	−
15	1000	44 ± 3	0.7 ± 0.1	101.0 ± 4.0	0.2 ± 0.05
15	500	33 ± 3	0.3 ± 0.1	85.0 ± 27.0	0.14 ± 0.05
70[b]	2000[b]	65 ± 23[b]	0.8 ± 0.1[b]	531 ± 30[b]	2.4 ± 0.2[b]

[a] FIM-1 (3 nM) fluorescence was measured in the presence of 3 nM PKCα after preincubation for 5 min with PS and then incubation for 300 s in the presence of TPA ("steady state" protocol), the TPA concentration ranging from 10 to 1360 nM. The Ca^{2+} effect was first studied in the absence of PS (A). Under these conditions, the best fit was obtained with a one-site model. When high amounts of PS were present in the medium (B), the dose−response curves were best fitted with a two-site model ($10^{-4} < p < 10^{-3}$). [b] These data are representative of two independent sources of PKCα . PKCα enzymes from Gibco and Calbiochem were assessed in three and two independent experiments, respectively, and the values are averages ± SD.

PS and 2 mM Ca^{2+}. We identified two TPA binding sites ($p < 10^{-4}$ when compared to a single-binding site model with the *F* test) with EC_{50} values of 70 ± 14 and 652 ± 106 nM (Figure 7A).

The PS concentration dependence of these two binding sites was studied, and we found that under 15 μM PS the amplitude of the fluorescence change of the lower-affinity binding site was under our measurement limit (Table 4). Therefore, we focused on the high-affinity binding site to measure its distinct PS dependence. The TPA EC_{50} values for this high-affinity site did not change in the range of 0.3−70 μM PS, but a clear 3-fold enhancement of the fluorescence amplitude was observed. Surprisingly, this high-affinity binding site remained unchanged on the soluble PKCα (in the absence of PS vesicles), showing a pre-existing and remarkably steady binding site for TPA on the enzyme (Table 4).

The Ca^{2+} concentration dependence (in the range of 0−1000 μM) of a high-affinity binding site was tested on both soluble and PS-bound PKCα (Table 4). No modulation of the EC_{50} value was observed. However, the amplitude of the fluorescence increase greatly depended on the presence of Ca^{2+} in the medium (9-fold increase in the absence of PS).

In conclusion, neither membrane association nor PS or Ca^{2+} concentrations significantly altered the EC_{50} value for TPA (Table 4) on this high-affinity site, but they both enhanced the corresponding amplitude of the fluorescence change.

The question arose as to whether this high-affinity TPA binding and the corresponding conformational change revealed by FIM-1 fluorescence in our experimental conditions were actually modulating the PKCα activity. This was subsequently verified by measuring PKC phosphorylating activity, keeping as close as possible the conditions used with the two methods. We added FIM-1 (3 nM) to PKC and measured the extent of TPA-dependent histone I phosphorylation by PKCα after incubation for 20 min at 30 °C (Figure 7B). The EC_{50} was 32.4 nM for the high-affinity site in the presence of 70 μM PS and 2 mM Ca^{2+}, a value close to that obtained above by FIM-1 fluorescence measurements. The low-affinity binding site was not studied with this method. By adding different FIM-1 concentrations (0, 3, and 7 nM) to PKCα before the histone I phosphorylation, we also verified that the high-affinity binding site was not altered (not shown).

Proteolysis by μ-Calpain. Most of the FIM-1 fluorescence changes described here were obtained from activation cofactors acting on the regulatory domain of PKCα. It was therefore interesting to check whether we could observe a fluorescence modification in the absence of the regulatory domain of the enzyme. We characterized the binding affinity of FIM-1 on the TPA-activated rat brain PKC and its corresponding purified trypsin-digested product, PKM. The two EC_{50} values (EC_{50-PKC} = 12.0 ± 0.4 nM and EC_{50-PKM} = 12.8 ± 0.5 nM) were notably similar with the same cooperativity, suggesting an unaltered binding site of FIM-1 on both proteins. Moreover, the emission intensity of the FIM-1−PKM complex decreased by 30% compared with that of the original FIM-1−PKC, showing that the regulatory domain had an enhancing influence on the fluorescence yield of the probe (Figure 8A).

Active PKCα is rapidly hydrolyzed by Ca^{2+}-dependent proteases such as μ-calpain (*32*). The sites of hydrolysis are at the hinge (V3) between the regulatory domain and the catalytic site, the extent of hydrolysis being strongly dependent on the protein conformation (*35*). Therefore, we used experimental conditions described by Cressman et al. (*35*) to generate PKM, the constitutively activated PKC catalytic domain, by μ-calpain hydrolysis of PKC. The fully activated enzyme [5 nM rat brain PKC, with 1 μM TPA, 14 μM PS, and 2.0 mM Ca^{2+} in 20 mM TRIS buffer (pH 7.4) at 25 °C] was incubated with 4.1 units of μ-calpain. The emission intensity decreased (Figure 8B), again suggesting the formation of another enzyme−probe complex with a lower quantum yield, possibly FIM-1−PKM. To verify whether there was no further degradation of the PKM by μ-calpain during the incubation period, we incubated (under experimental conditions similar to those mentioned above) purified rat brain PKM with 4.1 units of μ-calpain and found no change even after a relatively long 50 min incubation (Figure 8B). Only a fraction of the PKC was hydrolyzed by

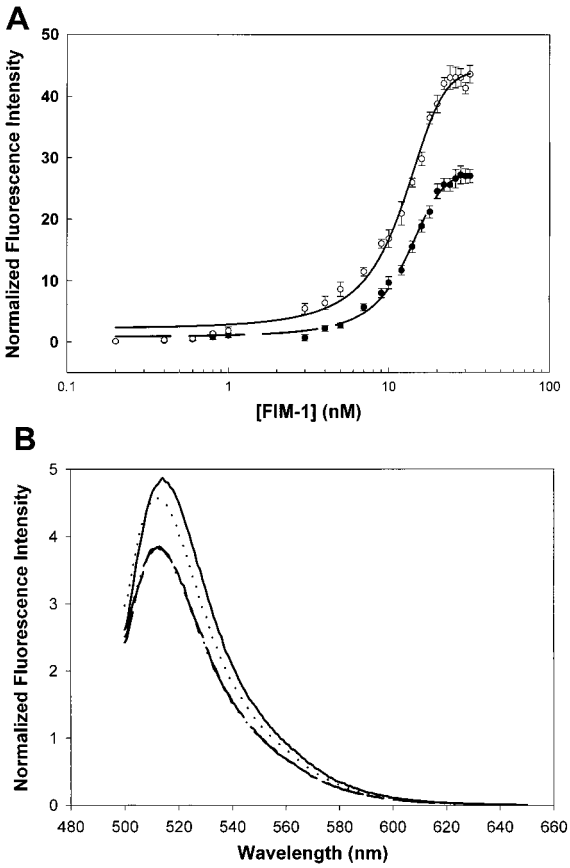

FIGURE 8: FIM-1 binding to PKM and PKCα. (A) FIM-1 binding affinities on rat brain PKCα and its trypsin-digested PKM form. FIM-1 at various concentrations was incubated in 20 mM TRIS buffer (pH 7.4) containing 14 μM PS, 1.5 mM Ca^{2+}, and 1 μM TPA at 25 °C for 5 min in the presence of 5 nM rat brain PKCα (solid line and ●) or 5 nM rat brain trypsin-digested PKM (dashed line and ●). For subsequent normalization, the I_1 values determined for 3 nM FIM-1 were used. EC_{50} for PKCα was 12.0 ± 0.4 nM, and for PKM 12.8 ± 0.5 nM. (B) Emission spectra of μ-calpain-hydrolyzed PKCα and purified trypsin-digested PKCα (PKMα) labeled with FIM-1. Rat brain PKCα (3 nM) was preincubated with 3 nM FIM-1 and 1 μM TPA for 30 min at 23 °C in 20 mM TRIS buffer (pH 7.4) containing 1 mM $CaCl_2$ and 14 μM PS vesicles. Then 4.1 units of μ-calpain was added for the proteolysis. The emission spectra were recorded before μ-calpain addition (—) and when no more spectral change occurred (e.g., 53 min after μ-calpain addition; ···). As a control, the FIM-1 spectrum was also recorded in the presence of PKMα in the same buffer without μ-calpain (— — —) and 53 min after the addition of μ-calpain (— · · · —). Note that these latter two spectra were virtually identical, indicating that PKMα was resistant to μ-calpain hydrolysis under our measurement conditions.

μ-calpain. In this case, the spectrum recorded after 50 min indicated a mixed population of both enzymes (e.g., around 65% PKC and 35% PKM; see Figure 8B).

The effect of μ-calpain on the FIM-1—PKCα complex was measured so the rate of proteolysis could be studied. FIM-1 (3 nM) and PKCα (3 nM) were mixed in the presence of 2 mM Ca^{2+} and 125 nM TPA and incubated with 70 μM PS vesicles at 25 °C for 30 min. Upon addition of 4.1 units of μ-calpain, the fluorescence intensity decreased (Figure 9) with a time constant of 2130 ± 20 s. This rate was strongly sensitive to μ-calpain concentration. Increasing the concentration of μ-calpain (6.15 units) increased the rate of fluorescence decrease, giving a new time constant of 637 ± 74 s (Figure 9 and Table 5).

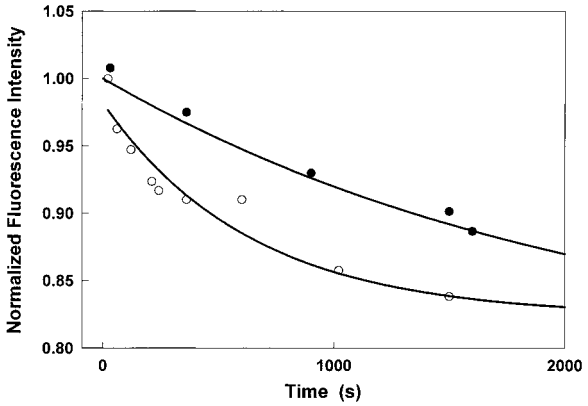

FIGURE 9: Comparison of the fluorescence decay of FIM-1-labeled PKCα induced by two different μ-calpain concentrations. A similar proteolysis procedure like that described in the legend of Figure 8 was used. Different amounts of μ-calpain were mixed into the observation cuvette at 25 °C. Full fluorescence spectra were recorded at given times and deconvoluted. The normalization factor was performed with the I_1 value measured at time zero in each experiment. The addition of μ-calpain [4.1 (●) or 6.15 units (○)] induced a fluorescence decay with a time constant depending on the protease concentration. Data points are the average of two series of two separate experiments.

Table 5[a]

[μ-calpain] (units/mL)	[TPA] (nM)	[PS] (μM)	FIM-1 fluorescence decay (time constant, min)
4.1	125	70	35.5 ± 0.5
6.15	125	70	10.6 ± 1.2
4.1	0	70	196.7 ± 10.0
4.1	620	70	21.4 ± 0.7
4.1	125	140	7.0 ± 0.5

[a] PKCα (0.25 μg/mL) and FIM-1 (3 nM) were incubated for 30 min at 25 °C with different amounts of TPA in 20 mM TRIS buffer containing 2 mM Ca^{2+} and 70 or 140 μM PS vesicles. Then 4.1 or 6.15 units/mL μ-calpain was added directly to the solution. Spectra were recorded and then analyzed. Time constants were calculated from the average of three independent series of two experiments.

Parallel measurements using the Western blot technique showed that the addition of μ-calpain (4.1 units) to 3 nM PKCα (in the presence of 70 μM PS, 125 nM TPA, and 2 mM Ca^{2+} at 25 °C) induced PKC hydrolysis with a time constant of 2136 ± 234 s and simultaneous PKM formation with the same rate (Figure 9A,B). This indicated that under our measurement conditions 4.1 units of μ-calpain hydrolyzed PKCα only at the hinge between the catalytic site and the regulatory domain, and no further degradation of PKM was observed. The similarity of PKCα hydrolysis rates determined by the Western blot technique and FIM-1 fluorescence validates the idea that the extent of PKC hydrolysis can be measured by the fluorescence technique.

Since it has been suggested that the hinge region is more sensitive to proteolysis when PKC is in a fully activated conformation (*34*), we measured the μ-calpain-induced fluorescence decrease with different TPA concentrations (absent or at 125 or 620 nM). A very slow decay rate was observed in the absence of TPA (Table 5), reflecting a rather weak proteolysis of PKC. Considering that the high concentrations of Ca^{2+} and PS alone without phorbol ester can induce a partially activated conformation of PKCα, where the hinge is freely accessible for the cleavage, we can assume that the observed fluorescence decay reflects the rate of

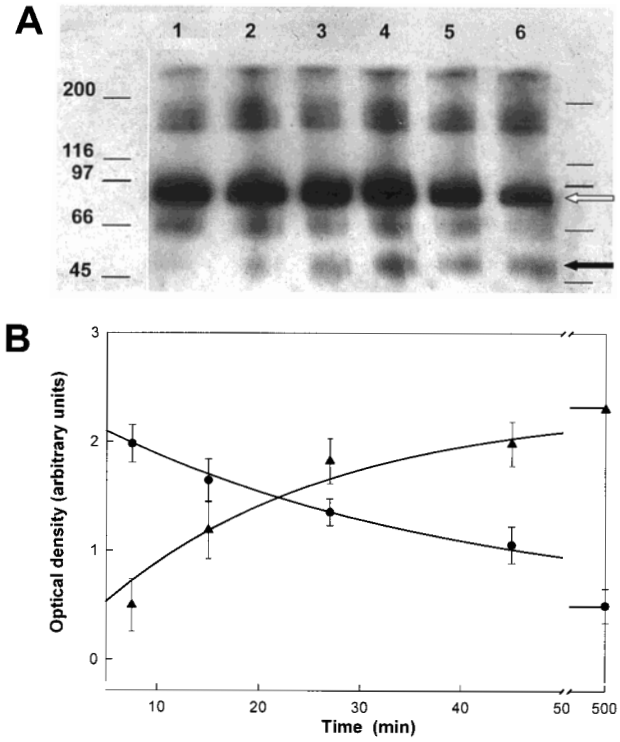

FIGURE 10: PKCα proteolysis by μ-calpain. (A) Western blot of PKCα during proteolysis by μ-calpain. PKCα (0.25 μg/mL) was preincubated with 125 nM TPA for 30 min at 25 °C in 20 mM TRIS buffer (pH 7.4) containing 2 mM $CaCl_2$ and 70 μM PS vesicles. Then 4.1 units of μ-calpain was added to start the proteolysis. Aliquots were taken at given intervals and quickly frozen at −23 °C. The samples were analyzed by SDS−PAGE. Western blots were obtained as described in Experimental Conditions: lane 1, 1.5 min; lane 2, 7.5 min; lane 3, 15 min; lane 4, 27 min; lane 5, 45 min; and lane 6, 8.5 h. PKCα and PKMα bands are denoted with white and black arrows, respectively. (B) Western blot quantification of PKCα proteolysis (●) and simultaneous PKM formation (▲) upon μ-calpain cleavage. The optical density was measured by computer image analysis. Data points are the average of four experiments ± SD.

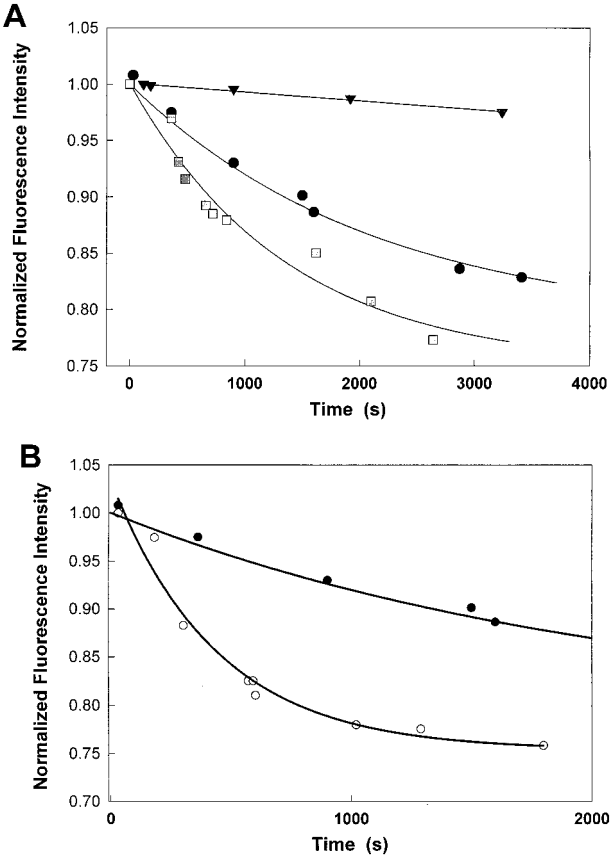

FIGURE 11: TPA and PS concentration dependence of PKCα proteolysis by μ-calpain. (A) PKCα (0.25 μg/mL) and FIM-1 (3 nM) were incubated for 30 min at 25 °C with different amounts of TPA [0 (▼), 125 (●), and 620 nM (□)] in 20 mM TRIS buffer containing 2 mM Ca^{2+} and 70 μM PS vesicles. Then 4.1 units of μ-calpain was mixed directly into the solution. Spectra were recorded at given times and analyzed. The calculated I_1 values were normalized by the I_1 value determined at time zero in each experiment. Incubation with various concentrations of TPA gave very different starting I_1 values, which cannot be seen after normalization. Data points are the average of three independent series of two experiments. (B) The incubation procedure was like that described for panel A except that the TPA concentration was fixed at 125 nM while the concentration of PS vesicles in the incubation buffer was either 70 (●) or 140 μM (○). The normalization was performed as described for panel A. Data points are the average of three separate experiments performed in duplicate.

hydrolysis by calpain. An increased TPA concentration, which induces a full activation of PKCα, sped considerably the observed decay and exhibited a strong TPA concentration dependence (Figure 11A and Table 5).

PKC activation by PS also plays an important role in controlling PKC proteolysis by μ-calpain (*35*). Doubling the PS concentration from 70 to 140 μM induced a huge 5-fold change in the time constant, from 35.5 ± 0.5 to 7.0 ± 0.5 min (Figure 11B and Table 5).

DISCUSSION

FIM-1 Characterization. As expected from previous studies (*31*, *36*), FIM-1 interacts with PKCα. We show that this interaction induces an increase in FIM-1 fluorescence intensity, which is partially reversed after subsequent addition of staurosporine, a competitive PKC inhibitor at the ATP binding site. The binding affinity of FIM-1 for PKCα remained rather steady when the measurement was performed under different activating conditions of PKC (Figure 2). Such a stable affinity has been previously described for staurosporine (*37*). More recently, Edwards and Newton (*25*) described only a weak shift in the ATP affinity for PKCβII upon phosphorylation of the protein, which triggers the PKC activation. The EC_{50} values which reflect the binding affinity of the probe for the enzyme were unchanged under conditions where PKC was not activated (e.g., PKCα in TRIS buffer alone), partially activated (in the presence of Ca^{2+} and/or PS), or fully activated (TPA in the presence of Ca^{2+} and/or PS). The observations presented here also agree with a previous report (*25*) showing that the ATP binding site is stable and cannot be perturbed by membrane association of the enzyme. Interestingly enough, the quantum yield of the probe when bound to the enzyme depends on the activation state of the enzyme. The fluorescence intensity increase was maximal in the presence of all the cofactors, PS, Ca^{2+}, and TPA, which are fully activating the enzyme. This fluorescence increase shows that FIM-1, which binds reversibly on the catalytic domain, is sensitive to different activation states of the enzyme and its microenvironment can be perturbed by the conformation changes of the regulatory half of PKCα. We can thus conclude that FIM-1 is a powerful probe for showing the difference in PKCα activation steps.

Our data analysis shows an apparently stable affinity of binding sites of FIM-1 for PKCα, whatever the measurement conditions are. A similar affinity was obtained by measuring an almost complete inhibition of the PKC phosphorylating activity in the presence of FIM-1. In the case of direct fluorescence measurements, the Hill coefficient was around 2 (see Table 2), which might indicate an allosteric effect between different sites. This observation agrees with Huang (*38*), who reported that there are two ATP-binding consensus sites in the C3 and C4 domains of PKCα and PKC*β* isoforms. These two sites exhibit the same affinity for ATP (*38*). The n_H value observed here, however, was close to 1.5 when measured by the extent of FIM-1 inhibition of PKCα activity. This slight discrepancy between the two measurements also reflects contradiction in the literature since according to Miyazaki et al. (*37*), who performed binding experiments with [^{3}H]staurosporine, there is a single ATP site on PKC. Hence, two possibilities could explain our findings: (i) as for ATP, there are two FIM-1 binding sites on PKCα, which have a positive allosteric interaction in agreement with Huang (*38*), or (ii) there is a dimeric form of PKCα under our experimental conditions. We observed dimeric bands in our Western blot experiments despite performing the experiments under denaturing conditions. However, the similar cooperativity observed for FIM-1 binding to PKC and to PKM makes this last hypothesis very unlikely.

Effect of Ca^{2+} on the PKC Conformation. Although previous studies reported a single Ca^{2+} binding site on PKC (*39*, *40*), structural studies (*41*) described two Ca^{2+} binding sites on the C2 PKC domain. Moreover, biochemical studies suggested different physiological effects on PKC activation for these sites (*23*). Our results agree with these findings since we determined two apparent sites for Ca^{2+} from our dose−response curve. The K_{Dapp} value for Ca^{2+} has been reported to be largely shifted toward higher values upon reduction of the phospholipid concentration (*22*, *39*). Our experimental conditions with low PS vesicle concentrations revealed two distinct Ca^{2+} binding sites with rather low affinities. These two binding sites, which had been previously suggested when PKC was lipid-bound and activated by phorbol ester and/or DAG (*23*), are detectable even on the partially activated PKCα since neither DAG nor phorbol ester was used in our experiments. The soluble PKC and membrane-bound PKC exhibit very different affinities for Ca^{2+} (*40*). This implies that the Ca^{2+} affinity for PKC is strongly modulated by the conformational status of the protein kinase.

PKC−TPA Interaction. FIM-1-labeled PKCα added to PS vesicles in the presence of Ca^{2+} exhibited a weak but fast (in the minute range) monoexponential fluorescence increase. Labeled and soluble PKC exhibited a weak and 10-fold slower monoexponential fluorescence increase after addition of TPA in the presence of Ca^{2+} and without PS vesicles. We observed that TPA addition in the presence of both Ca^{2+} and PS triggered a rise in fluorescence intensity best described by double-exponential kinetics (with time constants of 40−90 and 570−1300 s, respectively). In this case, the amplitude of the fluorescence change was dramatically enhanced and TPA concentration-dependent.

Since the observed fluorescence signal results from the combination of the different states of the fluorescently labeled enzyme, we are not able to detect directly a simple bimolecular step by this fluorescence measurement. Hence, several reaction steps must contribute to the complex fluorescence signal, including the conformational changes of the enzyme complex after TPA binding. We can only assess the most likely dominating steps and have a qualitative approach to this problem without elaborated calculation of the different models. Both rates, which describe the changes in the observed fluorescence signal, are TPA-dependent. Hence, the reaction step, which most likely triggers the observed kinetics, should be either the binding of TPA to the regulatory domain of the enzyme or the following conformational changes induced by this binding. Since the FIM-1 probe binds to the catalytic domain of the enzyme, the observed fluorescence change caused by TPA binding cannot be directly detected unless it causes a global conformational change of the protein.

Mosior and Newton (*16*) also reported double-exponential kinetics for the TPA−PKC*β*II interaction. The authors (*16*) used a binding assay, which did not allow them to measure data points before 19 min, while the fluorescence label technique enabled us to start to record within 10 s. This allowed us to detect a "rapid" component of the fluorescence change, which is completed within 5 min and therefore undetectable for biochemical binding assays. Thus, very likely, the two newly observed kinetic components described here are the resolution of the first binding kinetics previously reported by Mosior and Newton (*16*).

The rate of the "rapid component" depended on TPA concentration and was strongly modulated by PS, indicating that membrane association is an important factor in this process. The large effect of PS on the kinetic rates suggests that FIM-1−PKC fluorescence changes are dominated not just by TPA binding to the enzyme but also by a PS interaction with the newly formed enzyme complex after the first TPA binding. These PS-dependent fast kinetics can also reflect a conformational change of the C1 sequence induced by the modified PS binding site on the C2 domain of PKC, which makes the second TPA binding site on C1 sequence more accessible (*15*). We observed an almost 1 order of magnitude difference between the two rates. The small rate value of the slow kinetics may arise from the difference of two or several rates. Since this rate is also TPA- and PS-dependent, we can assume that the contributing steps are TPA binding or consecutive conformational changes driven by TPA binding on the membrane-associated enzyme.

Additional information was obtained as the amplitudes of the observed fluorescence changes were both TPA concentration-dependent. We determined two distinct changes, which can indicate two distinct binding sites for TPA on PKCα. The calculated EC_{50} values of TPA are very close to the binding affinities reported by Slater et al. (*14*, *18*), who described two phorbol ester binding sites using a phorbol-derived fluorescent probe and biochemical measurements. Molecular studies have described two cysteine-rich sequences on the regulatory domain of PKC (*8*−*12*), giving the possibility of two TPA binding sites.

We found that the high-affinity binding site is remarkably stable upon PS and Ca^{2+} modulation. Even on soluble PKCα, this binding site was determined to have similar high affinity. This shows that, although membrane association of PKCα is not an absolute requirement for phorbol ester binding (*18*), the kinetic rates of TPA binding can be modified by these

interactions. Furthermore, our results suggest that neither Ca^{2+} nor PS affected the high-affinity binding site of TPA on soluble or membrane-associated enzymes. However, the amplification of the fluorescence amplitude by these cofactors shows their involvement in a TPA-induced mechanism.

We observed a Ca^{2+}-independent high-affinity phorbol ester binding site, in agreement with the results of Quest and Bell (*10*). Ca^{2+} insensitivity of the TPA high-affinity binding site does not imply that there are no Ca^{2+}-induced small conformation changes, which can affect the PKC activity. However, there is indirect evidence of such a Ca^{2+}-independent activation of classical PKC isoforms by phorbol esters since numerous authors reported that Ca^{2+} chelation in the presence of phorbol esters only induced a partial PKC inactivation (*26*, *27*, *42*−*45*). Quest and Bell also reported that low-affinity phorbol ester binding could only be detected in the presence of the C2 calcium-binding domain on the protein. This might correspond to the low-affinity TPA binding site described here since PKCα includes the C2 domain. Our results on this site already support this last report since we observed a modulation of the low-affinity site by either Ca^{2+} or PS. This hypothesis however has to be confirmed with similar studies on Ca^{2+}-independent PKC isoforms.

Effect of μ-Calpain. We have shown that the FIM-1 fluorescence yield is greatly affected by the conformation of the PKCα regulatory domain since it is indirectly sensitive to Ca^{2+}, PS, and TPA, three agents regulating PKC activation states. It was therefore interesting to test the effect of μ-calpain since this protease hydrolyzes PKC at the hinge region between the catalytic domain and the regulatory region (*34*). Using μ-calpain, it was thus possible to generate PKMα, a kinase depleted from its regulatory domain and constitutively active (*34*, *35*). Although PKCα has been reported to be less sensitive to μ-calpain activity than other classical isoforms (*34*), we could observe a significant fluorescence decrease in the presence of μ-calpain. The PKMα−FIM-1 complex has a lower quantum yield than PKCα−FIM-1. We also observed that PKM was not further degraded by μ-calpain, which shows it is a substrate poorer than PKCα. Surprisingly, PKM exhibited the same affinity for the probe as PKC, suggesting a highly stable binding site, which was preserved after cleavage of the regulatory domain of the enzyme. Since Western blot experiments show parallel PKCα hydrolysis and PKMα formation, we could use our experimental conditions to study the process of hydrolysis of PKC by μ-calpain.

PKC hydrolysis by μ-calpain is of great physiological importance, and still there is scarce information about its kinetic properties and its modulation by DAG, phorbol esters, or PS. Our experiments show that the rate of PKCα hydrolysis by μ-calpain depends on the activated conformation of PKC itself. Numerous reports have been published on this topic (*13*, *46*−*50*). Using 125 nM TPA for PKC activation, we saturated the high-affinity binding site of TPA on PKCα. Increasing the TPA concentration 5-fold, we started to cause the low-affinity binding site to be occupied, and we were able to observe that the occupancy of this site modulates the conformation and the hydrolysis of PKCα. This change in TPA concentration induced a 2-fold change in the observed fluorescence decay rate. It implies that low-affinity and high-affinity binding sites induce distinct and active conformations of the enzyme. The difference between these two activated conformations probably involves the hinge region since they are differentially sensitive to proteolysis. Thus, FIM-1 appears to be an essential tool in structural studies of PKC hydrolysis since it allows temporal analysis of these processes with a great resolution, which was not yet available with classical biochemical methods. This tool will be used to study the process of calpain activation, and the sensitivity of the different PKC isoforms to hydrolysis.

In summary, the change in the PKCα−FIM-1 complex fluorescence upon activation of the enzyme appears to be specifically related to an interaction between the regulatory domain and the catalytic site of the protein. The probe exhibits a constant affinity for PKCα, whatever the incubation conditions are, suggesting a highly stable affinity of the ATP site on the enzyme. Our results also suggest the presence of two phorbol ester binding sites on the enzyme and a global conformational change of the enzyme. TPA binding on the regulatory domain also affects the conformation of the catalytic domain. The high-affinity TPA binding was remarkably stable and not perturbed by membrane association of the enzyme. As shown here, the occupancy of these two binding sites corresponds to different protein conformations according to TPA dose−response curves and hydrolysis experiments. We also show that the TPA−PKC interaction can be well described by biexponential kinetics with independent amplitudes. The rapid component of the TPA binding mainly reflects a PS−PKC−TPA interaction and should bring more insights to signal transduction studies. The rate of PKCα proteolysis by μ-calpain, which is strongly magnified by PS, indicates a dominant role for membrane association. To test the general importance of membrane association of PKC in the activation and proteolytic processes, other isoforms of PKC have to be studied. FIM-1 appears to be a powerful probe, which can detect discrete and/or minor PKC conformational changes and is able to reveal interactions between the regulatory and the catalytic domains of the enzyme.

ACKNOWLEDGMENT

We are grateful to Dr. J. L. Rodeau for developing the spectral analysis computer program, his constant support, and fruitful discussions. We are also indebted to Drs. A. Feltz and G. Duportail for their advice and to Dr. F. McKenna for carefully reading the manuscript.

REFERENCES

1. Nishizuka, Y. (1992) *Science 258*, 607−614.
2. Bell, R. M., and Burns, D. J. (1991) *J. Biol. Chem. 266*, 4661−4664.
3. Ashendel, C. L. (1985) *Biochim. Biophys. Acta 822*, 219−242.
4. Newton, A. C. (1993) *Annu. Rev. Biophys. Biomol. Struct. 22*, 1−25.
5. Ono, Y., Fujii, T., Igarashi, K., Kuno, T., Kikkawa, U., and Nishizuka, Y. (1989) *Proc. Natl. Acad. Sci. U.S.A. 86*, 4868−4871.
6. Hubbard, S. R., Bishop, W. R., Kirschmeier, P., George, S. J., Cramer, S. P., and Hendrickson, W. A. (1991) *Science 254*, 1776−1779.
7. Quest, A. F. G., Bloomenthal, J., Bardes, E. S. G., and Bell, R. M. (1992) *J. Biol. Chem. 267*, 10193−10197.
8. Quest, A. F., Bardes, E. S., and Bell, R. M. (1994) *J. Biol. Chem. 269*, 2953−2960.

9. Quest, A. F., Bardes, E. S., and Bell, R. M. (1994) *J. Biol. Chem. 269*, 2961−2970.
10. Quest, A. F., and Bell, R. M. (1994) *J. Biol. Chem. 269*, 20000−20012.
11. Zhang, Q., Frankel, P., and Foster, D. A. (1995) *Cell Growth Differ. 6*, 1367−1373.
12. Burns, D. J., and Bell, R. M. (1991) *J. Biol. Chem. 266*, 18330−18338.
13. Slater, S. J., Kelly, M. B., Taddeo, F. J., Rubin, E., and Stubbs, C. D. (1994) *J. Biol. Chem. 269*, 17160−17165.
14. Slater, S. J., Ho, C., Kelly, M. B., Larkin, J. D., Taddeo, F. J., Yeager, M. D., and Stubbs, C. D. (1996) *J. Biol. Chem. 271*, 4627−4631.
15. Oancea, E., and Meyer, T. (1998) *Cell 95*, 307−318.
16. Mosior, M., and Newton, A. C. (1996) *Biochemistry 35*, 1612−1623.
17. Luo, J. H., Kahn, S., O'Driscoll, K., and Weinstein, I. B. (1993) *J. Biol. Chem. 268*, 3715−3719.
18. Slater, S. J., Taddeo, F. J., Mazurek, A., Stagliano, B. A., Milani, S. K., Kelly, M. B., Ho, C., and Stubbs, C. D. (1998) *J. Biol. Chem. 273*, 23160−23168.
19. Al, Z., and Cohen, C. M. (1993) *Biochem. J. 296*, 675−683.
20. Dutil, E. M., Keranen, L. M., DePaoli-Roach, A. A., and Newton, A. C. (1994) *J. Biol. Chem. 269*, 29359−29362.
21. Orr, J. W., and Newton, A. C. (1994) *J. Biol. Chem. 269*, 27715−27718.
22. Keranen, L. M., Dutil, E. M., and Newton, A. C. (1995) *Curr. Biol. 5*, 1395−1403.
23. Keranen, L. M., and Newton, A. C. (1997) *J. Biol. Chem. 272*, 25959−25967.
24. Bornancin, F., and Parker, P. J. (1996) *Curr. Biol. 9*, 1114−1123.
25. Edwards, A. S., and Newton, A. C. (1997) *J. Biol. Chem. 272*, 18382−18390.
26. Bazzi, M. D., and Nelsestuen, G. L. (1988) *Biochemistry 27*, 6776−6783.
27. Bazzi, M. D., and Nelsestuen, G. L. (1989) *Biochemistry 28*, 9317−9323.
28. Pap, E. H. W., van den Berg, P. A. W., Borst, J. W., and Wisser, A. J. W. G. (1995) *J. Biol. Chem. 270*, 1254−1260.
29. Bastiaens, P. I. H., and Jovin, T. M. (1996) *Proc. Natl. Acad. Sci. U.S.A. 93*, 8407−8412.
30. Toullec, D., Pianetti, P., Coste, H., Bellevergue, P., Grand-Perret, T., Ajakane, M., Baudet, V., Boissin, P., Boursier, E., Loriolle, F., Duhamel, L., Charon, D., and Kirilovsky, J. (1991) *J. Biol. Chem. 266*, 15771−15781.
31. Chen, C. S., and Poenie, M. (1993) *J. Biol. Chem. 268*, 15812−15822.
32. Slater, S. J., Kelly, M. B., Taddeo, F. J., Ho, C., Rubin, E., and Stubbs, C. D. (1994) *J. Biol. Chem. 269*, 4866−4871.
33. McGuigan, J. A., Lüthi, D., and Buri, A. (1991) *Can. J. Physiol. Pharmacol. 69*, 1733−1749.
34. Kishimoto, A., Mikawa, K., Hashimoto, K., Yasuda, I., Tominaga, M., Kuroda, T., and Nishizuka, Y. (1989) *J. Biol. Chem. 264*, 4088−4092.
35. Cressman, C. M., Mohan, P. S., Nixon, R. A., and Shea, T. B. (1995) *FEBS Lett. 367*, 223−227.
36. de Barry, J., Kawahara, S., Takamura, K., Janoshazi, A., Kirino, Y., Olds, J., Lester, D. S., Alkon, D. L., and Yoshioka, T. (1997) *Exp. Cell Res. 234*, 115−124.
37. Miyazaki, A., Kitamura, Y., and Nomura, Y. (1993) *Neurochem. Int. 22*, 455−464.
38. Huang, K. P. (1989) *Trends Neurosci. 12*, 425−432.
39. Luo, J. H., and Weinstein, I. B. (1993) *J. Biol. Chem. 268*, 23580−23584.
40. Mosior, M., and Epand, R. M. (1994) *J. Biol. Chem. 269*, 13798−13805.
41. Shao, X., Davletov, B. A., Sutton, R. B., Sudhof, T. C., and Rizo, J. (1996) *Science 273*, 248−251.
42. Kazanietz, M. G., Krausz, K. W., and Blumberg, P. M. (1992) *J. Biol. Chem. 267*, 20878−20886.
43. Dimitrijevic, S. M., Ryves, W. J., Parker, P. J., and Evans, F. J. (1995) *Mol. Pharmacol. 48*, 259−267.
44. Wender, P. A., Irie, K., and Miller, B. L. (1995) *Proc. Natl. Acad. Sci. U.S.A. 92*, 239−243.
45. Kazanietz, M. G., Areces, L. B., Bahador, A., Mischak, H., Goodnight, J., Mushinski, J. F., and Blumberg, P. M. (1993) *Mol. Pharmacol. 44*, 298−307.
46. Suzuki, T., Okumura-Noji, K., Ogura, A., Tanaka, R., Nakamura, K., and Kudo, Y. (1992) *Biochem. Biophys. Res. Commun. 189*, 1515−1520.
47. Nixon, R. A., Saito, K. I., Grynspan, F., Griffin, W. R., Katayama, S., Honda, T., Mohan, P. S., Shea, T. B., and Beermann, M. (1994) *Ann. N.Y. Acad. Sci. 747*, 77−91.
48. Eto, A., Akita, Y., Saido, T. C., Suzuki, K., and Kawashima, S. (1995) *J. Biol. Chem. 270*, 25115−25120.
49. Shea, T. B., Cressman, C. M., Spencer, M. J., Beermann, M. L., and Nixon, R. A. (1995) *J. Neurochem. 65*, 517−527.
50. Hrabetova, S., and Saktor, T. C. (1996) *J. Neurosci. 16*, 5324−5333.

BI990427M